DOI: 10.2478/auom-2025-0017
An. Şt. Univ. Ovidius Constanţa **Vol. 33(2),2025, 27–43**

On the zero-free region and the distribution of zeros of the prime zeta function

Igoris Belovas, Rugilė Čepaitytė and Martynas Sabaliauskas

Abstract

The prime zeta function is one of the most under-researched varieties of the class. Very little is known about the irregular distribution of its zeros. The presented study aims - albeit partially - to fill the gap in our understanding of the subject. We consider the zero-free region of the prime zeta function and verify statistically certain conjectures regarding the distribution patterns of the zeroes of the prime zeta function.

1 Introduction

Zeta functions are important analytical tools employed to address underlying problems of number theory. Some of these functions, e.g., the Riemann zeta function, the Hurwitz zeta function, the Lerch zeta function, Dirichlet L-functions or zeta functions of the Selberg class, have been extensively studied, while others have received minimal attention.

A perfect example of such a function is the prime zeta, one of the most under-researched varieties of the class. The behavior of the prime zeta function may hold significant insights into the underlying properties of prime numbers and their distribution. It is important to note that while all known nontrivial zeros of the Riemann zeta function are located on the critical line (the famous Riemann hypothesis states that all the nontrivial zeros belong to the line $\sigma = 1/2$), the zeros of the prime zeta function are scattered not only in the

Key Words: prime zeta function, zeta function zeros, zero-free region.
2010 Mathematics Subject Classification: Primary 11M41; Secondary 11M99.
Received: 07.10.2024
Accepted: 28.02.2025

critical strip ($0 < \sigma \leqslant 1$) but also in its outside (see Section 2). Thus, their distribution is more sophisticated. Very little is known about the zero-free region of the prime zeta function.

Let $s = \sigma + it$ be a complex variable and $\mathbb{P}$ stand for the set of prime numbers. The prime zeta function, denoted by $\zeta_{\mathbb{P}}(s)$, is a function of a complex variable defined as the following Dirichlet series,

$$\zeta_{\mathbb{P}}(s) = \sum_{p \in \mathbb{P}} \frac{1}{p^s},$$

in the half-plane $\sigma > 1$ and its analytic continuation in the critical strip $0 < \sigma \leqslant 1$. The prime zeta function can be expressed in terms of the Riemann zeta function,

$$\zeta_{\mathbb{P}}(s) = \sum_{n=1}^{\infty} \frac{\mu(n)}{n} \log \zeta(ns), \tag{1}$$

where $\mu(n)$ stands for the Möbius function. Formula (1) provides an analytic continuation of the prime zeta function to the critical strip $0 < \sigma \leqslant 1$. Landau and Walfisz showed that the prime zeta function cannot be continued to the half-plane $\sigma \leqslant 0$ (see [5]). This is due to the clustering of singular points along the imaginary axis emanating from the nontrivial zeros of the zeta function on the critical line. On the real axis, the prime zeta function has singularities at reciprocals of square-free positive integers. In this study, we consider the zero-free region of the prime zeta function and statistically verify certain conjectures regarding the distribution of its zeros.

The paper is organized as follows. The first part is the introduction. In Section 2, the theorem about the zero-free region of the prime zeta function is proved. In Section 3, we formulate some conjectures regarding the properties of the zeros of the prime zeta function. Chapter 4 is dedicated to algorithms for calculating the prime zeta function. Chapter 5 covers the process of searching for zeros. In Chapter 6, we study numerically the conjectures regarding the distribution of zeros of the prime zeta function.

Throughout this paper, $U \times V$ stands for the Cartesian product of sets U and V, and $\mathbb{U}(0,1)$ stands for the standard uniform distribution. All limits in the paper, unless specified, are taken as $t \to \infty$.

2 The zero-free region of the prime zeta function

The distribution of zeros of the prime zeta function is highly irregular. In contrast to the Riemann zeta function, with its nontrivial zeros lying on the critical line, the zeros of the prime zeta function are scattered in the complex plane without an apparent regular pattern. They belong both to the critical strip and its outside. It can be noted, however, that the density of the zeros increases while approaching the imaginary axis, though not uniformly, cf. the plot of 10318 zeros we have found in the rectangle $0.1 < \sigma < 1.65$, $0 < t < 10^4$ (Fig. 1).

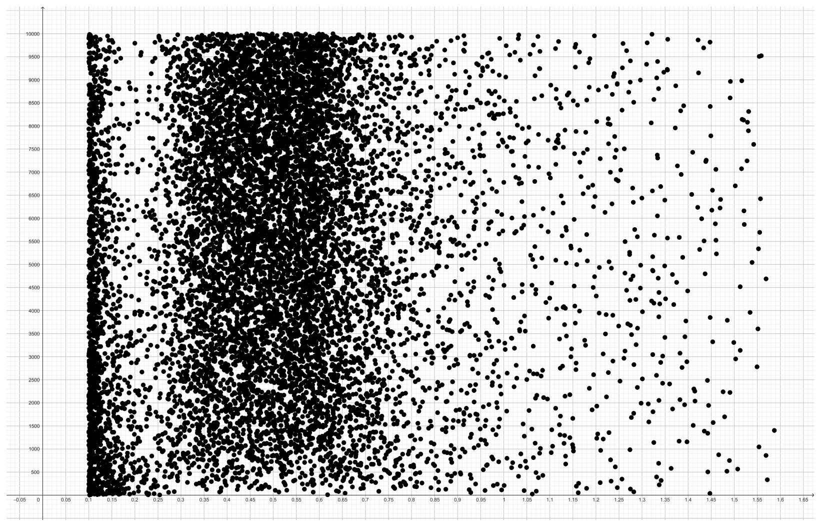

Figure 1: Zeros of $\zeta_{\mathbb{P}}(s)$ in the rectangle $0.1 < \sigma < 1.65$, $0 < t < 10^4$. The number of zeros is 10318.

We can see that the density of zeros tends to zero while σ increases. Indeed, there exists a constant σ_0 such that the half plane $\sigma > \sigma_0$ is the zero-free region. The following theorem gives the value of σ_0.

Theorem 1. *The prime zeta function has no zeros in the half-plane $\sigma > \sigma_0$. Here $\sigma_0 = 1.77954465354699...$ is the zero of the function $U(\sigma) = 2^{1-\sigma} - \zeta_{\mathbb{P}}(\sigma)$.*

First, we prove an auxiliary lemma describing the function's $U(\sigma)$ behavior.

Lemma 1. *Let the function $U(\sigma)$ be defined as above and $\sigma_1 = 2.18$, then*

$$\begin{cases} U'(\sigma) > 0, & \text{if} \quad 1 < \sigma \leqslant \sigma_1, \\ U(\sigma) > 0, & \text{if} \quad \sigma \geqslant \sigma_1. \end{cases}$$

Proof. Let us consider the first statement of the lemma. Calculating the derivative, we receive, for $1 < \sigma \leqslant \sigma_1$,

$$U'(\sigma) = -\frac{\log 2}{2^\sigma} + \sum_{p \geqslant 3} \frac{\log p}{p^\sigma} > -\frac{\log 2}{2^\sigma} + \frac{\log 3}{3^\sigma} + \frac{\log 5}{5^\sigma} + \frac{\log 7}{7^\sigma}$$

$$> \underbrace{-\frac{\log 2}{2^\sigma} + 3\sqrt[3]{\frac{\log 3}{3^\sigma}\frac{\log 5}{5^\sigma}\frac{\log 7}{7^\sigma}}}_{:=A_1(\sigma)} > 0.$$

Indeed, $A_1(\sigma) > 0$ follows from the inequality

$$\left(\frac{2}{\sqrt[3]{105}}\right)^\sigma > \frac{\log 2}{3\sqrt[3]{\log 3 \log 5 \log 7}} = 0.1530466... , \quad \sigma \leqslant \sigma_1,$$

yielding us the first statement of the lemma.

Next, let $\sigma_2 = 2.46$ and $\sigma \geqslant \sigma_2$. Considering the function $U(\sigma)$ we get

$$U(\sigma) = \frac{1}{2^\sigma} - \sum_{p \geqslant 3} \frac{1}{p^\sigma} > \frac{1}{2^\sigma} - \sum_{n=3}^{\infty} \frac{1}{n^\sigma}.$$

Applying the Euler–Maclaurin summation formula,

$$\sum_{n=a}^{b} f(n) = \int_a^b f(x)dx + \frac{f(b) + f(a)}{2} + \frac{f'(b) - f'(a)}{12} + R_2,$$

where the remainder term

$$|R_2| \leqslant \frac{1}{12}\int_a^b \left|f^{(2)}(x)\right| dx,$$

we receive

$$\sum_{n=3}^{\infty} \frac{1}{n^\sigma} \leqslant \left(\frac{3}{\sigma - 1} + \frac{1}{2} + \frac{\sigma}{18}\right)\frac{1}{3^\sigma},$$

thus

$$U(\sigma) > \frac{1}{2^\sigma} - \left(\frac{3}{\sigma - 1} + \frac{1}{2} + \frac{\sigma}{18}\right)\frac{1}{3^\sigma} = \frac{1}{3^\sigma}\underbrace{\left(\left(\frac{3}{2}\right)^\sigma - \frac{3}{\sigma - 1} - \frac{1}{2} - \frac{\sigma}{18}\right)}_{:=A_2(\sigma)} > 0,$$

$$\sigma \geqslant \sigma_2.$$

Indeed, considering the derivatives of the function $A_2(\sigma)$, we get

$$\begin{aligned} A_2'(\sigma) &= \left(\frac{3}{2}\right)^\sigma \log\frac{3}{2} + \frac{3}{(\sigma-1)^2} - \frac{1}{18} \\ A_2^{(2)}(\sigma) &= \left(\frac{3}{2}\right)^\sigma \log^2\frac{3}{2} - \frac{6}{(\sigma-1)^3}, \\ A_2^{(3)}(\sigma) &= \left(\frac{3}{2}\right)^\sigma \log^3\frac{3}{2} + \frac{18}{(\sigma-1)^4} > 0. \end{aligned}$$

Thus $A_2'(\sigma)$ is convex. Solving the equation $A_2^{(2)}(\sigma) = 0$ we express its unique minimum point using the Lambert W function,

$$\sigma_{\min} = \arg\min_\sigma A_2'(\sigma) = 1 + \frac{3}{\log(3/2)} W\left(\frac{1}{3}\sqrt[3]{4\log\frac{3}{2}}\right) = 3.1631259788\ldots .$$

Noticing that

$$A_2'(\sigma_{\min}) = \min_\sigma A_2'(\sigma) > 0,$$

we conclude that $A_2(\sigma)$ is a monotonic (increasing) function, positive in the interval $\sigma \geqslant \sigma_2$, since $A_2(\sigma_2) > 0$.

Next, let us consider the behavior of the function $U(\sigma)$ if $\sigma_1 \leqslant \sigma \leqslant \sigma_2$. From the definition of the function $U(\sigma)$ we get

$$U(\sigma) = \frac{1}{2^\sigma} - \frac{1}{3^\sigma} - \frac{1}{5^\sigma} - \sum_{p\geqslant 7}\frac{1}{p^\sigma} > \frac{1}{2^\sigma} - \frac{1}{3^\sigma} - \frac{1}{5^\sigma} - \sum_{n=7}^{\infty}\frac{1}{n^\sigma}.$$

Applying the Euler–Maclaurin summation formula, we receive

$$\sum_{n=7}^{\infty}\frac{1}{n^\sigma} \leqslant \left(\frac{7}{\sigma-1} + \frac{1}{2} + \frac{\sigma}{42}\right)\frac{1}{7^\sigma},$$

thus, for $\sigma_1 \leqslant \sigma \leqslant \sigma_2$,

$$\begin{aligned} U(\sigma) &> \frac{1}{2^\sigma} - \frac{1}{3^\sigma} - \frac{1}{5^\sigma} - \left(\frac{7}{\sigma-1} + \frac{1}{2} + \frac{\sigma}{42}\right)\frac{1}{7^\sigma} \\ &= \frac{1}{7^\sigma}\underbrace{\left(\left(\frac{7}{2}\right)^\sigma - \left(\frac{7}{3}\right)^\sigma - \left(\frac{7}{5}\right)^\sigma - \frac{7}{\sigma-1} - \frac{1}{2} - \frac{\sigma}{42}\right)}_{:=B(\sigma)} > 0. \end{aligned}$$

Indeed, we have

$$B_1(\sigma) := \left(\frac{7}{2}\right)^\sigma \geqslant \left(\frac{7}{2}\right)^a + \left(\frac{7}{2}\right)^a \left(\log\frac{7}{2}\right)(\sigma - a),$$

since $B_1(\sigma)$ is a convex function (hence its graph lies above the tangent). Next, the functions $B_2(\sigma), B_3(\sigma), B_4(\sigma)$ are concave, thus secant lines, connecting points $(a, B_j(a))$ and $(b, B_j(b))$, lie below the functions,

$$B_2(\sigma) := -\left(\frac{7}{3}\right)^{\sigma} \geqslant B_2(a) + \frac{B_2(b) - B_2(a)}{b-a}(\sigma - a),$$
$$B_3(\sigma) := -\left(\frac{7}{5}\right)^{\sigma} \geqslant B_3(a) + \frac{B_3(b) - B_3(a)}{b-a}(\sigma - a),$$
$$B_4(\sigma) := -\frac{7}{\sigma - 1} \geqslant B_4(a) + \frac{B_4(b) - B_4(a)}{b-a}(\sigma - a).$$

Here $a = \sigma_1$ and $b = \sigma_2$. Combining the above inequalities, we receive

$$\begin{aligned} B(\sigma) \geqslant & \left(\frac{7}{2}\right)^{a} + \left(\frac{7}{2}\right)^{a} \left(\log \frac{7}{2}\right)(\sigma - a) - \frac{1}{2} - \frac{\sigma}{42} \\ & + (B_2 + B_3 + B_4)(a) + \frac{(B_2 + B_3 + B_4)(b) - (B_2 + B_3 + B_4)(a)}{b-a}(\sigma - a) \\ & = P\sigma + Q. \end{aligned}$$

Calculating the constants, we obtain $P = 16.46873847...$ and $Q = -35.46121108...$. Thus $B(\sigma_1) > 0$, yielding us the second statement of the lemma. □

Now, we can turn to the proof of Theorem 1.

Proof. First we note that

$$|\zeta_{\mathbb{P}}(s)| = \left| \frac{1}{2^s} + \frac{1}{3^s} + \frac{1}{5^s} + ... \right| > \frac{1}{2^\sigma} - \frac{1}{3^\sigma} - \frac{1}{5^\sigma} - ... = 2^{1-\sigma} - \zeta_{\mathbb{P}}(\sigma) = U(\sigma).$$

Next we prove that $U(\sigma) > 0$ for $\sigma > \sigma_0$. Indeed, by Lemma 1, the function $U(\sigma)$ is increasing for $1 < \sigma \leqslant \sigma_1$. Next, $U(1.77) < 0$ and $U(1.78) > 0$, thus we have a root $1.77 < \sigma_0 < 1.78$. Moreover, since, by Lemma 1, the function $U(\sigma)$ is positive for $\sigma \geqslant \sigma_1$, the root (note that we can calculate it numerically with any necessary precision) is unique. □

Remark 1. *Let* $M = 200000$ *and define*

$$\sigma_T = \max_{|t|<T} \{ \ \sigma \mid \zeta_{\mathbb{P}}(\sigma) = 0 \ \}, \tag{2}$$

then we receive

$$\sigma_M = 1.682628788045196... \ .$$

Thus, the result of Theorem 1 can not be refined by more than $\Delta = 0.097$.

3 Conjectures

The intricate behavior of the prime zeta function obstructs the analytical investigation of its properties. Under these circumstances the application of the methods of experimental mathematics and mathematical statistics appears to be promising. We can put forward (and later test and falsify) the following conjectures:

Conjecture 1. *The estimate for the zero-free plane given by Theorem 1 can not be improved, that is, if σ_T is defined as above (see (2)), then*

$$\lim_{T\to\infty} \sigma_T = \sigma_0. \tag{3}$$

Conjecture 2. *Let $0 < \gamma < \sigma_0$ and*

$$L_\gamma(x,T) = \#\{s \mid \zeta_{\mathbb{P}}(s) = 0,\ \sigma > \gamma,\ 0 < t/T < x\},$$

then the imaginary parts of the zeros of the prime zeta function $\Im s$ are distributed uniformly, i.e., for $\gamma \geqslant 1$ and $0 < x < 1$, we have

$$\lim_{T\to\infty} \frac{L_\gamma(x,T)}{L_\gamma(1,T)} \Rightarrow \mathbb{U}(0,1). \tag{4}$$

Conjecture 3. *Let $0 < \gamma < \sigma_0$ and*

$$M_\gamma(T) = \#\{s \mid \zeta_{\mathbb{P}}(s) = 0,\ \sigma > \gamma,\ 0 < t < T\},$$

then there are positive constants c and C (maybe depending on γ), such that the inequality

$$cT < M_\gamma(T) < CT \tag{5}$$

holds, for $\gamma > 1$ and T large enough. The weaker proposition is $M_1(T) = O(T)$.

Remark 2. *The behavior of the function $N_\beta(T)$,*

$$N_\beta(T) = \#\{s \mid \zeta_{\mathbb{P}}(s) = 0,\ 0 < \beta < \sigma < \sigma_0, 0 < t < T\}$$

is more complicated, the limiting distribution seems to be bimodal (see Section 6).

Remark 3. *It remains unclear whether there is any regularity in the distribution of the zeros of $\zeta_{\mathbb{P}}(s)$, akin to the $\log\zeta(s)$ (cf. Section XI.8 in [6]).*

Indeed, the behaviour of $\zeta_{\mathbb{P}}(s)$ is closely connected to the log-zeta function,

$$\log \zeta(s) - \zeta_{\mathbb{P}}(s) = \sum_{n=2}^{\infty} \frac{1}{n} \sum_{p\in\mathbb{P}} \frac{1}{p^{ns}}, \qquad \sigma > 1/2.$$

Estimating the difference, we obtain

$$|\log \zeta(s) - \zeta_{\mathbb{P}}(s)| \leqslant \underbrace{\sum_{n=2}^{\infty} \frac{\zeta_{\mathbb{P}}(n\sigma)}{n}}_{:=G(\sigma)} < \underbrace{\frac{\zeta_{\mathbb{P}}(2\sigma)}{2} + \frac{\zeta_{\mathbb{P}}(3\sigma)}{3} + \frac{\zeta_{\mathbb{P}}(4\sigma)}{4}\left(1 + \frac{1}{2^{\sigma}} + \frac{1}{2^{2\sigma}}\right)}_{<\zeta_{\mathbb{P}}(2\sigma)(2^{-1}+2^{-\sigma-1})}.$$

The function $G(\sigma)$ is convex and monotonically decreasing, and for $\sigma > 1$ we have $|R(s)| \leqslant G(\sigma) < G(1) = \gamma - B_1 = 0.31571845205...$. Here, γ and B_1 stand for the Euler–Mascheroni and the Meissel–Mertens constants respectively.

4 Calculating the prime zeta function

We implemented and examined ten earlier proposed algorithms to calculate the prime zeta function and introduced some modifications. We also utilized two built-in algorithms for the prime zeta function as benchmarks. All the approaches are outlined in this section and stored in [7]. Note that the computational difficulties increase tremendously as $\sigma \to 0$ and $t \to \infty$.

- *Algorithm 1: Prime_Zeta_Froberg1.* The first algorithm under consideration was proposed by Fröberg [4]. It is comprised of two main blocks: (1) the Riemann zeta function calculation block (`"ZETA1"`) and (2) the prime zeta function calculation block.

- *Algorithm 2: Prime_Zeta_Mobius1.* This algorithm relies on (1), employing the Möbius function and the Riemann zeta function. The Möbius function for $n \in \mathbb{N}$, is calculated as follows,

$$\mu(n) = \begin{cases} 1 & \text{if } n = 1, \\ 0 & \text{if } n \text{ contains a square factor,} \\ (-1)^q & \text{if } n \text{ is the product of } q \text{ different prime factors.} \end{cases}$$

  For the calculation of the Riemann zeta function, we took the `ZETA1` algorithm.

- *Algorithm 3: Prime_Zeta_Cohen1.* Note that $\log\zeta(ns) = O(2^{-n\sigma})$. Hence, (1) converges rapidly enough to allow precise calculations. Cohen, however, recommended (see [2]) a more refined approach: to compute the series's partial sum first and use the Riemann zeta function expansion only for the remainder term. Indeed, let us set

  $$\zeta_{p>A}(s) = \zeta(s) \prod_{p\leqslant A} \left(1 - \frac{1}{p^s}\right),$$

  then, we can modify (1) in the following way,

  $$\zeta_{\mathbb{P}}(s) = \sum_{p\leqslant A} \frac{1}{p^s} + \sum_{n=1}^{\infty} \frac{\mu(n)}{n} \log\zeta_{p>A}(ns).$$

  Since $\log\zeta_{p>A}(ns) = O(A^{-n\sigma})$, the series converges much faster than the original series if A is not too small. The optimal value of A depends on the desired accuracy and is selected empirically (values from 20 to 100 are reasonable if high precision is necessary [2]).

- *Algorithm 4: Prime_Zeta_MobiusPython.* Replacing the `ZETA1` block with the built-in *Python* function `"zeta"`, we receive a modified version of Algorithm 2, now referred to as Algorithm 4.

- *Algorithm 5: Prime_Zeta_CohenPython.* By applying the above modification to Algorithm 3, we obtain Algorithm 5.

- *Algorithm 6: Python's primezeta.* Additionally, we have utilized *Python*'s built-in function `"primezeta"` for calculating the prime zeta function.

- *Algorithm 7: Prime_Zeta_FrobergX.* This modification uses the *EMB*-algorithm (proposed in [1]) for the calculation of the Riemann zeta function. We use this block, named `ZETAX`, to replace `ZETA1` in Algorithm 1, thus attaining Algorithm 7.

- *Algorithm 8: Prime_Zeta_CohenX.* Replacing `ZETA1` block with `ZETAX` in Algorithm 3, we receive the next modification, named Algorithm 8.

- *Algorithm 9: Prime_Zeta_Froberg_Fast.* Replacing `ZETA1` block in Algorithm 1 with block `zetafast`, containing Fischer's *Zetafast* algorithm (see [3]), we receive Algorithm 9.

- *Algorithm 10: Prime_Zeta_Mobius_Fast.* Replacing `ZETA1` with `zetafast` in Algorithm 2, we obtain Algorithm 10.

- *Algorithm 11: Prime_Zeta_Cohen_Fast.* Replacing `ZETA1` with `zetafast` in Algorithm 3, we receive Algorithm 11.
- *Algorithm 12: Wolfram's Cohen-Lenstra-Martinet.* In Wolfram's *Mathematica*, one can access the prime zeta function using the `PrimeZetaP` function. This function is built into *Mathematica* and leverages efficient algorithms, including the *Cohen-Lenstra-Martinet* approach, to compute the values of the prime zeta function. Note that *Wolfram* `PrimeZetaP` is faster than *Python*'s built-in function *primezeta* and provides the most accurate results; that is why we have used *Wolfram's* results as a benchmark.

To determine the most efficient approach, we standardized the accuracy of the algorithms to the same number of decimal places. Next, we subdivided the domains of interest into smaller rectangles S_i, generating for every rectangle S_i a set of 100 random points, and calculated the prime zeta function values at each point. Using the above algorithms, we executed three test trials. Note that in different parameter regions, the efficiency of the algorithms varies in the following way:

1. In the range $(\sigma, t) \in (0.1, 1) \times (10^2, 10^4)$, Algorithm 11 (**Cohen Fast**) exhibited the best computation time.
2. In the range $(\sigma, t) \in (0.1, 0.3) \times (10^1, 10^2)$, Algorithm 8 (**CohenX**) was the most efficient.
3. In the range $(\sigma, t) \in (1, 1.78) \times (10^3, 10^4)$, Algorithm 6 (**Python Primezeta**) provided the best performance.
4. In the remaining domains, Algorithm 7 (**FrobergX**) outperformed other competitors.

The benchmarking experiments were conducted using *Python* 3.12.1 on a *Windows* 11 operating system, running on a single core of an **AMD Ryzen 9 5950X** CPU with 32 GB RAM. Each random value of the prime zeta function was taken over 100 uniformly distributed values, and the average computation time in seconds was recorded. The corresponding results are illustrated in Figure 2.

5 The calculation of zeros of the prime zeta function

We use a bivariate target function and the differential evolution algorithm for global optimization to find the zeros of the prime zeta function. The prime zeta function exhibits significant irregularity (see Figure 3). This irregularity makes

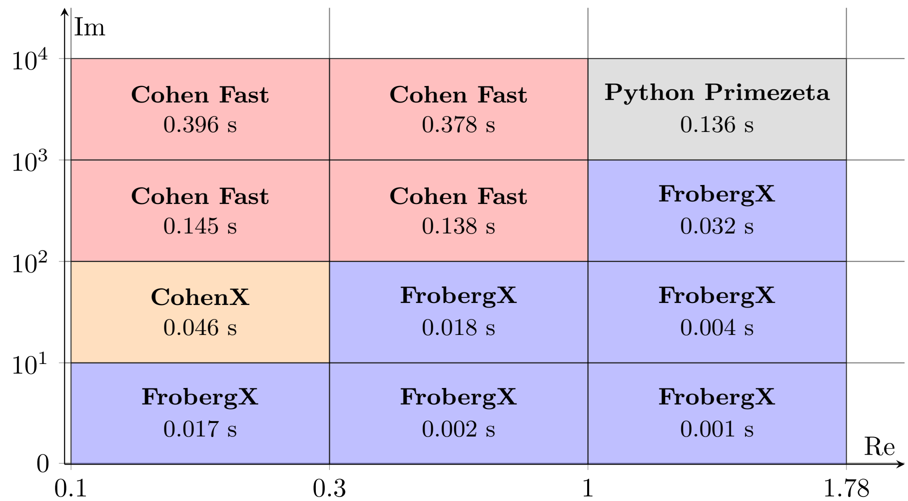

Figure 2: The diagram of the most efficient algorithms for specific domains (the average calculation time of a single prime zeta function value is given).

it infeasible to search for its zeros using currently available tools. To address the challenge, we employ a bivariate target function, the squared modulus of the prime zeta function,

$$F(\sigma, t) = |\zeta_{\mathbb{P}}(s)|^2 = (\Re\zeta_{\mathbb{P}}(s))^2 + (\Im\zeta_{\mathbb{P}}(s))^2. \tag{6}$$

By squaring the modulus of the prime zeta function, we smooth our target function, thereby facilitating optimization. The target function surface is visualized in Figure 4 (note that the blue dots correspond to the minima). A 2D plot of these zeros is given in Figure 5.

The task of searching for zeros is now equivalent to the problem of finding the minima of the target function. An alternative - well suited for the verification of the optimization - approach relies on the examination of intersection points of the curves $\Im\zeta_{\mathbb{P}}(s) = \Re\zeta_{\mathbb{P}}(s)$ with the zero-plane.

Given that the target function $F(\sigma, t)$ has multiple local optima (i.e., it is multi-modal), we applied the global optimization methods. The differential evolution algorithm for global optimization, specifically from the *scipy.optimize* (ver. 1.11.4) Python library, has been found to be the most suitable for our task. We employed three approaches to improve the calculation time. First is parameter fine-tuning (to perform faster in particular domains). Second, originally implemented in Python, the Cohen Fast algorithm was rewritten in C++, accelerating the computation of prime zeta

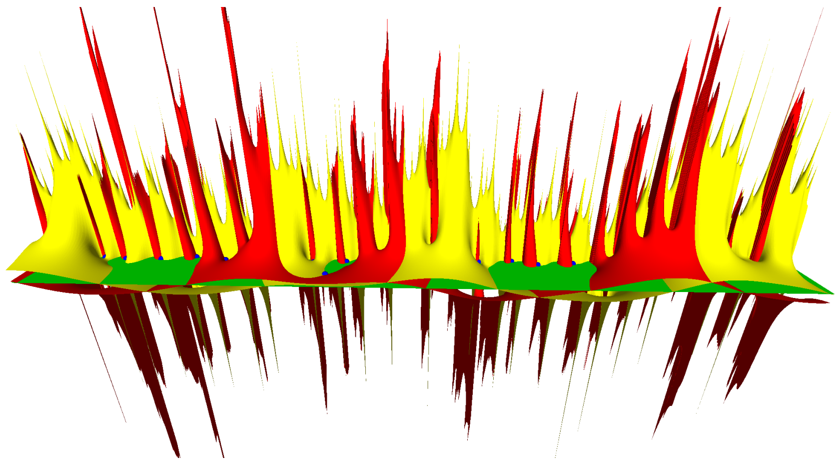

Figure 3: The real surface of $\zeta_{\mathbb{P}}(s)$ is yellow, the imaginary surface is red, the complex plane is green, the zeros are blue, $(\sigma, t) \in (0.1; 2) \times (9980; 10000)$.

values approximately 9 times. Using the *Cython* (ver. 3.0.6) library, we created a module that allows the Cohen Fast C++ implementation to be seamlessly integrated into the Python environment. Third, we achieved an additional speedup of approximately 20 times by parallelizing the algorithm using *Python*'s multiprocessing module. By applying these optimizations and utilizing all 32 threads of the **AMD Ryzen 9 5950X** CPU, we were able to compute the 10,318 zeros presented in Figure 1 in less than a week.

To ensure that no significant quantities of zeros were missed, we examined the intervals between previously identified zeros. Each interval between two consecutive zeros was divided into ten parts, and the optimization algorithms were rerun. We noticed that the computational time increases exponentially, as $\sigma \to 0$. This phenomenon is closely related to the conjecture that the density of zeros also grows exponentially as $\sigma \to 0$. Given the limited timeframe, this fact restricted our domain to $\sigma \in (0.1; \sigma_0)$. The prime zeta function zeros database we have compiled is stored in [7].

Remark 4. *Visualizations are important for a deeper understanding of the sophisticated behavior and properties of the prime zeta function. By graphically representing surfaces and curves associated with* $\zeta_{\mathbb{P}}(s)$*, we can identify unobvious patterns, singularities, and characteristics of the function. This visual approach not only aids in the intuitive grasp of the function's dynamics but also facilitates the communication of complex mathematical ideas to a broader audience. Furthermore, these visualizations can serve as a foundation for future research, providing a visual context for hypotheses and guiding the development of new techniques. See the following online links with interactive*

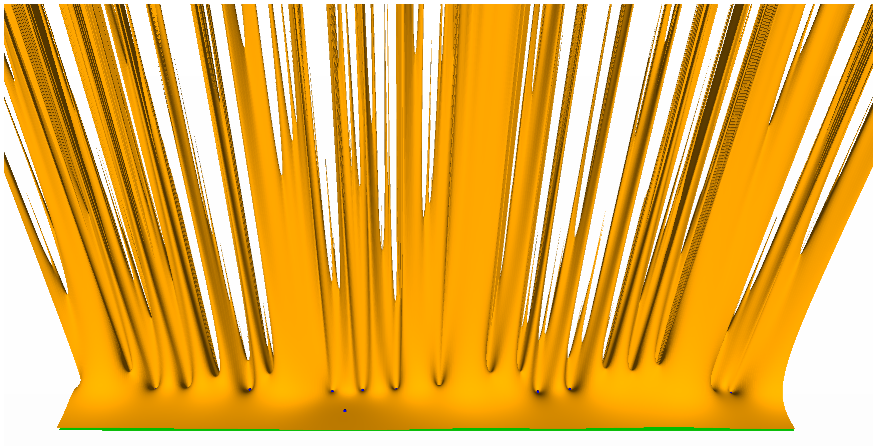

Figure 4: $|\zeta_{\mathbb{P}}(s)|^2$ in the rectangle $(0.1; 1.4) \times (9980; 10000)$.

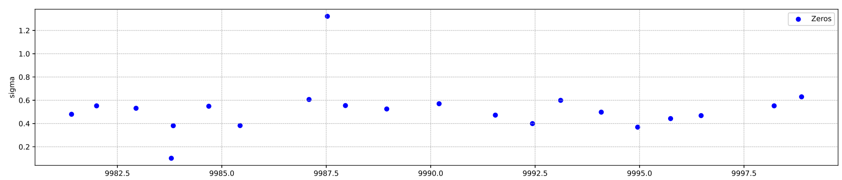

Figure 5: Zeros in the rectangle $(0.1; 1.4) \times (9980; 10000)$.

3D views:

- *Visualization of real and imaginary $\zeta_{\mathbb{P}}(s)$ surfaces:* ***https://skfb.ly/oUMnn***.
- *Visualization of real $\zeta_{\mathbb{P}}(s)$ surface:* ***https://skfb.ly/oUMns***.
- *Visualization of intersections of real and imaginary $\zeta_{\mathbb{P}}(s)$ surfaces:* ***https://skfb.ly/oUMIP***.
- *Visualization of $|\zeta_{\mathbb{P}}(s)|$:* ***https://skfb.ly/oUMny***.
- *Visualization of the target function* ***https://skfb.ly/oUMHZ***.

6 Properties of the distribution of zeros of the prime zeta function

We identified a total of 10318 zeros within the rectangle $S_4 = (0.1; \sigma_0) \times (0; 10^4)$ (see Figure 1). Next, we proceed with the statistical analysis and visualization of the empirical data. Through various graphical representations, we aim to elucidate the underlying patterns and trends present in the data. Additionally, we will test our hypotheses to validate the statistical significance of the observed results. These analyses will form the foundation for our subsequent analytical research.

Besides the scatter plot, another way to have a quick and insightful glimpse is to look at the data in a histogram form. A histogram showing the distribution of zeros by σ is given in Figure 6 (cf. Figure 1).

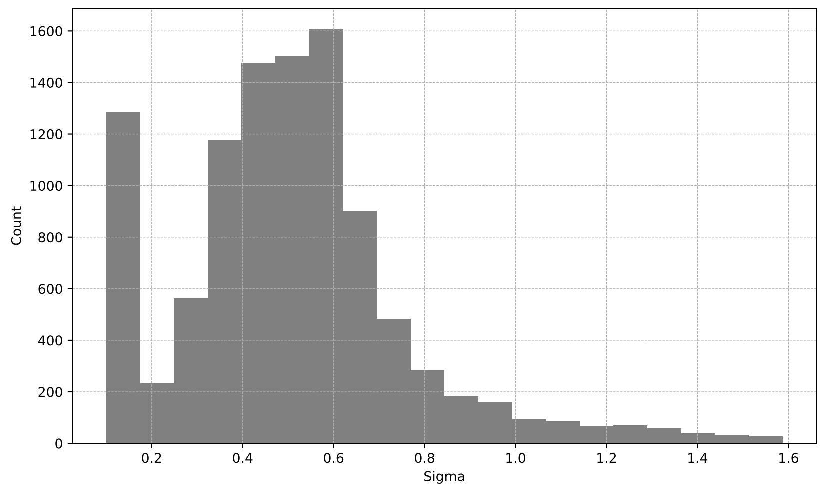

Figure 6: Histogram of $\zeta_{\mathbb{P}}(s)$ zeros distribution by σ, $s \in S_4$.

We observe that the majority of zeros is concentrated within the interval $(0.3; 0.7)$, with a pronounced peak in the histogram at $\sigma \approx 0.6$ and another significant peak near the left boundary. Beyond the critical strip $0 < \sigma \leqslant 1$, the occurrence of zeros becomes increasingly rare. The mean value (0.503) is slightly higher than the median (0.493); thus the distribution appears to be right-skewed. Next, we turn to Conjecture 2 (4) and Conjecture 3 (5) to statistically analyze the distribution of the imaginary parts of the zeros of the prime zeta function.

Conjecture 2.

We applied Kolmogorov, Anderson-Darling, and Cramér-von Mises tests to falsify the hypotheses of uniformity of the imaginary parts of the zeros of the prime zeta function. The results support the conjecture outside the critical strip (see. Table 1).

Table 1: Testing the hypotheses of the uniformity of the imaginary parts of the zeros of the prime zeta function in different half-planes for $T = 10^4$. The significance level $\alpha = 0.05$.

Half-plane	Test	Statistic	Critical value	Result
	Kolmogorov	0.037	0.013	Rejected
$\sigma > 0.1$	Anderson-Darling	39.890	2.492	Rejected
	Cramér-von Mises	7.330	0.461	Rejected
	Kolmogorov	0.020	0.026	Not rejected
$\sigma \geq 0.61$	Anderson-Darling	2.832	2.492	Rejected
	Cramér-von Mises	0.414	0.461	Not rejected
	Kolmogorov	0.015	0.027	Not rejected
$\sigma \geq 0.62$	Anderson-Darling	1.644	2.492	Not rejected
	Cramér-von Mises	0.212	0.461	Not rejected
	Kolmogorov	0.011	0.063	Not rejected
$\sigma > 1$	Anderson-Darling	0.057	2.492	Not rejected
	Cramér-von Mises	0.008	0.461	Not rejected

However, for $\gamma = 0.1$ (i.e., we have $\sigma > 0.1$), the conjecture is rejected. The conjecture begins to fail, starting at $\gamma \approx 0.61$. Moreover, it is conclusively rejected within the critical strip, $0.1 < \sigma < 1$. Thus, there is strong evidence that Conjecture 2 with $\sigma > 1$ cannot be rejected. However, to strictly prove the hypothesis, a further analytical study is required.

Conjecture 3.

Let $\gamma = 1$ in (5), then we have

$$M_1(T) = \#\{s \mid \zeta_{\mathbb{P}}(s) = 0,\ \sigma > 1,\ 0 < t < T\}.$$

Do there exist positive constants c_1 and C_1, such that the inequalities

$$c_1 T < M_1(T) < C_1 T,$$

hold for T large enough? We can see (cf. Figure 7) that numerical experiments conducted for $T < 10^4$ comply with the conjecture.
Moreover, we can indicate such constants $\hat{b}_1$ and $\hat{B}_1$, that the inequalities

$$k_1\, T + \hat{b}_1 < M_1(T) < k_1\, T + \hat{B}_1.$$

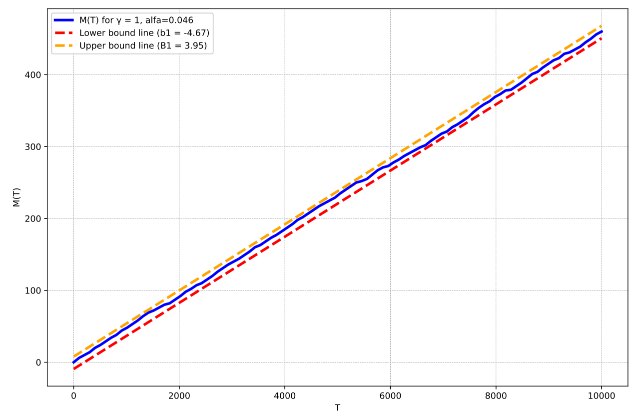

Figure 7: $M_1(T)$ plot for $T \in (0; 10^4)$ and its line bounds.

hold. Here, the slope and intercepts of the line bounds are

$$k_1 = 0.046, \quad \hat{b}_1 = -4.667, \quad \hat{B}_1 = 3.949.$$

Next, considering the case $\gamma = 0.1$ and $T < 10^4$, we obtained the following slope and intercepts of the line bounds, $k_{0.1} = 1.05$, $\hat{b}_{0.1} = -290$, $\hat{B}_{0.1} = 50$.

A visual representation of $M_{0.1}(T)$ with its upper and lower bounds is given in Figure 8. Note, however, that the apparent curvature of $M_{0.1}(T)$ hints that

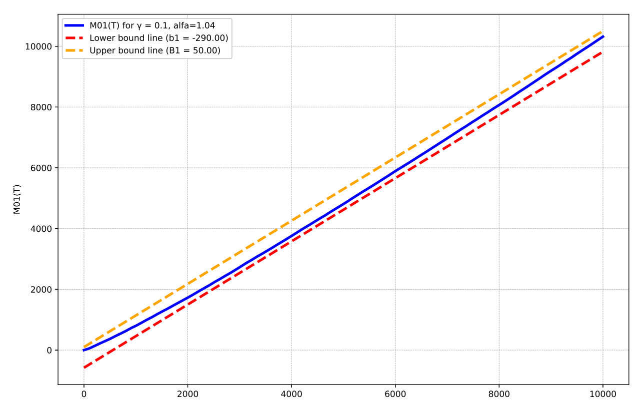

Figure 8: $M_{0.1}(T)$ plot for $T \in (0; 10^4)$ and its line bounds

the conjecture is false in the critical strip.

Acknowledgments

The authors would like to thank the anonymous reviewer for carefully reading the manuscript and providing constructive comments and suggestions, which have helped to improve the papers quality.

References

[1] I. Belovas, M. Sabaliauskas, L. Kuzma, *Series with binomial-like coefficients for the investigation of fractal structures associated with the Riemann zeta function*, Fractal and fractional, 6(6:300), 1–21, (2022). `https://doi.org/10.3390/fractalfract6060300`

[2] H. Cohen, *High precision computation of Hardy-Littlewood constants*, 1998 (preprint), `https://oeis.org/A221712/a221712.pdf`

[3] K. Fischer, *The Zetafast algorithm for computing zeta functions*, arXiv 2017, `https://arxiv.org/abs/1703.01414`

[4] C.-E. Fröberg, *On the prime zeta function*, Nordisk Tidskr. Informations-behandling (BIT), **8**(3): 187-202 (1968). `https://doi.org/10.1007/BF01933420`

[5] E. Landau, A. Walfisz, *Über die Nichfortsetzbarkeit einiger durch Dirichletsche Reihen definierter Funktionen*, Rend. Circ. Math. Palermo, **44**: 82–86 (1920).

[6] E. C. Titchmarsh, *The Theory of the Riemann Zeta-Function*, 1986, 2nd Edition, Oxford.

[7] I. Belovas, R. Čepaitytė, M. Sabaliauskas, *Prime Zeta Zeros*, 2024. `https://github.com/akatasis/prime-zeta-zeros`

Igoris Belovas,
Faculty of Mathematics and Informatics,
Vilnius University,
LT-04812 Vilnius, Lithuania.
Email: Igoris.Belovas@mif.vu.lt

Rugilė Čepaitytė,
Faculty of Mathematics and Informatics,
Vilnius University,
LT-04812 Vilnius, Lithuania.
Email: R.Cepait@gmail.com

Martynas SABALIAUSKAS,
Faculty of Mathematics and Informatics,
Vilnius University,
LT-04812 Vilnius, Lithuania.
Email: Martynas.Sabaliauskas@mif.vu.lt